Journal of Biomolecular NMR, **17:** 305–310, 2000.
KLUWER/ESCOM

NMR detection of side chain–side chain hydrogen bonding interactions in $^{13}C/^{15}N$-labeled proteins

Aizhuo Liu*, Weidong Hu, Ananya Majumdar, Michael K. Rosen & Dinshaw J. Patel
Cellular Biochemistry & Biophysics Program, Box 557, Memorial Sloan-Kettering Cancer Center, 1275 York Avenue, New York, NY 10021, U.S.A.

Received 28 April 2000; Accepted 22 May 2000

Key words: FKBP12, NMR detection, sensitivity enhancement, side chain–side chain hydrogen bonds

Abstract

We describe the direct observation of side chain–side chain hydrogen bonding interactions in proteins with sensitivity-enhanced NMR spectroscopy. Specifically, the remote correlation between the guanidinium nitrogen $^{15}N^{\epsilon}$ of arginine 71, which serves as the hydrogen donor, and the acceptor carboxylate carbon $^{13}CO_2{}^{\gamma}$ of aspartate 100 in a 12 kDa protein, human FKBP12, is detected via the *trans*-hydrogen bond $^{3h}J_{N\epsilon CO2\gamma}$ coupling by employing a novel HNCO-type experiment, soft CPD-HNCO. The $^{3h}J_{N\epsilon CO2\gamma}$ coupling constant appears to be even smaller than the average value of backbone $^{3h}J_{NC'}$ couplings, consistent with more extensive local dynamics in protein side chains. The identification of *trans*-hydrogen bond *J*-couplings between protein side chains should provide useful markers for monitoring hydrogen bonding interactions that contribute to the stability of protein folds, to alignments within enzyme active sites and to recognition events at macromolecular interfaces.

Introduction

Direct detection of spin–spin scalar couplings between nuclei of hydrogen donor and acceptor moieties in nucleic acids (Dingley and Grzesiek, 1998; Pervushin et al., 1998; Dingley et al. 1999; Majumdar et al., 1999a,b; Hennig and Williamson, 2000; Liu et al., 2000a), as well as in proteins (Cordier and Grzesiek, 1999; Cordier et al., 1999; Cornilescu et al. 1999a,b; Wang et al., 1999; Liu et al., 2000b; Meissner and Sørensen, 2000), has provided a new approach for monitoring hydrogen bonds and critical parameters for the characterization of structure and dynamics of biological macromolecules in solution by NMR.

The scalar couplings in proteins between the backbone amide nitrogen and carbonyl carbon nucleus, $^{3h}J_{NC'}$, as well as between the amide proton and carbonyl carbon nucleus, $^{2h}J_{NC'}$, of two residues involved in a N-H$\cdots$O=C hydrogen bond are of comparable magnitude and generally smaller than 1 Hz (Cordier and Grzesiek, 1999; Cordier et al., 1999; Cornilescu et al., 1999a). These observations are in agreement with the recent quantum chemical calculations of the magnitude of scalar couplings between atoms across the hydrogen bond (Dingley et al., 1999; Scheurer and Brüschweiler, 1999). In proteins, backbone–backbone hydrogen bonds are exclusively formed with the amide nitrogen as a hydrogen donor and the carbonyl carbon as a hydrogen acceptor and are most conveniently detected via *trans*-hydrogen bond $^{3h}J_{NC'}$ couplings by performing HNCO-type experiments (Kay et al., 1990; Grzesiek and Bax, 1992). On the other hand, a wider variety of donor–acceptor combinations is possible for hydrogen bonds involving side chains. Although hydrogen bonds involving amino acid side chains in a protein are not as ubiquitous as those involving the backbone, they do play a key role in stabilizing structures of polypeptides and protein–nucleic acid complexes. Most importantly, they are often crucial in the regulation of enzymatic reactions (Jeffrey and Saenger, 1991). Hydrogen bonding interactions involving side chains are expected to be generally weaker than the cor-

*To whom correspondence should be addressed. E-mail: aizhuo@sbnmr1.ski.mskcc.org

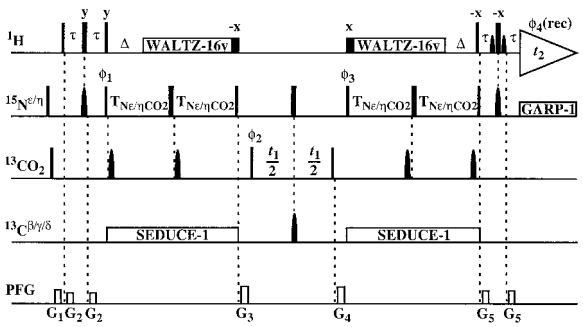

Figure 1. The pulse sequence of the soft 2D CPD-H(N)CO experiment that is used for the direct detection of protein side chain–side chain hydrogen bonds through *trans*-hydrogen bond $^{3h}J_{N\epsilon/\eta CO2\gamma}/^{3h}J_{N\epsilon/\eta CO2\delta}$ couplings between arginine guanidinium $^{15}N^{\epsilon/\eta}$ nitrogen and aspartate/glutamate carboxylate $^{13}CO_2$ carbon spins. Narrow and wide rectangular black bars indicate non-selective 90° and 180° pulses, respectively. Unless indicated otherwise, the pulses are applied with phase x. The ^1H, ^{15}N, and ^{13}C carrier frequencies are set at 4.77 ppm (water), 77.1 ppm (in the middle of arginine guanidinium $^{15}N^{\epsilon}$ and $^{15}N^{\eta}$ chemical shifts and 7.0 ppm upfield from $^{15}N^{\epsilon}$), and 181.0 ppm (aspartate/glutamate side chain carbonyl $^{13}CO_2$), respectively. The non-selective proton pulses are applied using a 47.2 kHz field strength. The selective ^1H 90° pulses, indicated with black shaped bars, used for water flip-back (Grzesiek and Bax, 1993) are rectangular pulses of duration 1.7 ms. Proton decoupling is achieved using the WALTZ-16 (Shaka et al., 1983) sequence succeeded or preceded by water flip-back pulses at 3.6 kHz field strength. The ^{15}N pulses are applied with a field strength of 6.1 kHz and ^{15}N decoupling using the GARP-1 (Shaka et al., 1985) sequence with 1.0 kHz is applied during acquisition. The arginine guanidinium $^{15}N^{\epsilon/\eta}$ selective inversion pulses indicated with shaped black bars are applied with the I-BURP-2 (Geen and Freeman, 1991) profile and 1.9 ms pulse length at 77.1 ppm to efficiently cover all of the $^{15}N^{\epsilon/\eta}$ chemical shifts but minimize the excitation of amides. The non-selective $^{13}CO_2$ carbon pulses are applied at 18.5 kHz field strength and the corresponding selective 180° pulses are applied with the Gaussian profile truncated at 5% amplitude having 101 μs pulse length. Arginine side chain $^{13}C\delta$ decoupling is achieved by using the WALTZ-16 sequence with phase modulated pulses having the SEDUCE-1 (McCoy and Mueller, 1992) profile (250 μs 90° pulse length) applied at 40.0 ppm. The aspartate/glutamate $^{13}C^{\beta/\gamma}$ selective 180° pulse in the middle of the $^{13}CO_2$ t_1 evolution time is also applied with the Gaussian profile truncated at 5% amplitude having 101 μs pulse length and the off-resonance effect is compensated by adjusting the phase of the $^{13}CO_2$ 90° pulse at the end of the t_1 period. The delays employed are : $\tau = 2.2$ ms, $\Delta = 5.5$ ms, and $T_{N\epsilon/\eta CO2} = 46.5$ ms for optimal observation of arginine guanidinium $^{15}N^{\epsilon}$-related correlation and $\Delta = 2.75$ ms for optimal observation of arginine guanidinium $^{15}N^{\eta}$-related correlation. The phase cycling scheme used is: ϕ_1 = x, −x; ϕ_2 = 2(x), 2(−x); ϕ_3 = 4(x), 4(−x); ϕ_4(rec) = x, −x, −x, x, −x, x, x, −x. Quadrature detection in the $\omega_1(^{13}C)$ dimension is achieved using States-TPPI (Marion et al., 1989) phase cycling of ϕ_2. The durations and strengths of the z-axis pulsed field gradients (PFG) employed are: G_1 = (1.5 ms, 20 G/cm), G_2 = (0.5 ms, 7 G/cm), G_3 = (0.8 ms, 10 G/cm), G_4 = (0.8 ms, 13 G/cm), G_5 = (0.3 ms, 17 G/cm). Magnetization begins on the arginine guanidino $^1H^{\epsilon/\eta}$, and is transferred to the attached $^{15}N^{\epsilon/eta}$ via the 'soft' INEPT step. *Figure 1.* (continued). The arginine $^{15}N^{\epsilon/\eta}$ magnetization is then partially transferred to the hydrogen bond linked aspartate/glutamate carboxylate carbon, $^{13}CO_2{}^{\gamma/\delta}$, via the *trans*-hydrogen bond $^{3h}J_{N\epsilon/\eta CO2\gamma}$ or $^{3h}J_{N\epsilon/\eta CO2\delta}$ coupling through the 'long-range' $^{15}N^{\epsilon/\eta}\rightarrow{}^{13}CO_2{}^{\gamma/\delta}$ defocusing period. Throughout the transfer, band-selective decoupling is applied to the arginine side chain $^{13}C^{\delta}$. This period, $2 \times T_{N\epsilon CO2}$, is set to $2/^1J_{N\epsilon C\zeta} = 93.0$ ms for optimal refocusing of the $^1J_{N\epsilon C\zeta} \approx 21.5$ Hz coupling. Subsequently, the $^{13}CO_2{}^{\gamma/\delta}$ magnetization is frequency-labeled during the t_1 evolution period, and then transferred back to the remote arginine guanidino $^1H^{\epsilon/\eta}$–$^{15}N^{\epsilon/\eta}$ proton for detection via the same pathway.

responding backbone–backbone interactions because side chains are generally involved in more extensive local dynamics (Fischer et al. 1998). Indeed, the point has been confirmed by the observation of backbone amide to side chain carboxyl hydrogen bonds for a small immunoglobulin binding domain (56 residues) of streptococcal protein G (Cornilescu et al., 1999b) and human FKBP12 (Liu et al., 2000c), although the *trans*-hydrogen bond $^{2h}J_{NN}$ scalar coupling constant between imidazole ^{15}NH nitrogens of the His24-His119 pair in apomyglobin was measured as large as 10 Hz (Hennig and Geierstanger, 1999). Detection of hydrogen bonds of protein side chains thus represents a challenge that requires the successful design of NMR experiments tailored to specific donor–acceptor moieties.

In this paper, we report the direct observation of the N^{ϵ}-H···O=C^{γ} hydrogen bonding interaction of the Arg 71–Asp 100 salt bridge in a 12 kDa protein, human FKBP12 (Harding et al., 1989; Siekierka et al., 1989; Rosen et al., 1990), via the three-bond $^{3h}J_{N\epsilon CO2\gamma}$ coupling between the arginine guanidinium nitrogen $^{15}N^{\epsilon}$ and aspartate carboxylate carbon $^{13}CO_2{}^{\gamma}$.

Experimental and results

To detect this extremely small coupling, we have developed a new sensitivity-enhanced HNCO-type experiment, soft CPD-HNCO, which bears two novel features in comparison with the conventional CT-HNCO experiment (Grzesiek and Bax, 1992). First, band-selective composite-pulse decoupling (CPD) applied to the arginine side chain $^{13}C^{\delta}$ (40–45 ppm) is employed during the entire $^{15}N^{\epsilon/\eta}\leftrightarrow{}^{13}CO_2{}^{\gamma/\delta}$ defocusing/refocusing periods in order to quench *J*-coupled mediated $^1H^{\delta}$-$^{13}C^{\delta}$ dipole–dipole (DD) relaxation (Liu, 1999; Liu et al., 2000b,d). Protein side

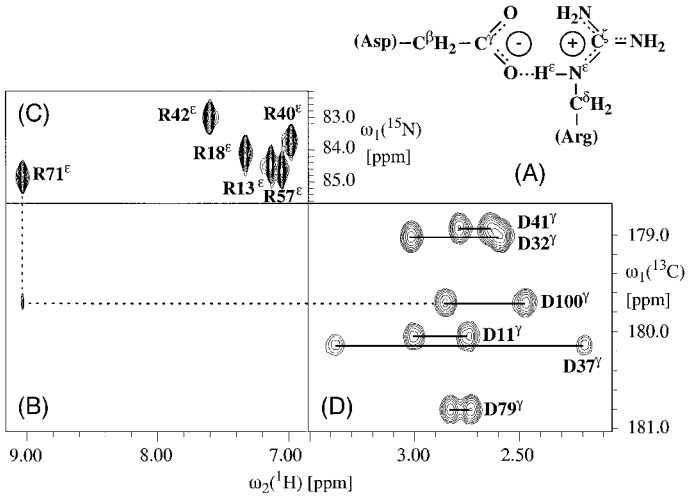

Figure 2. (A) Schematic representation of the hydrogen bond between the arginine 71 guanidinium $N^{\epsilon}H^{\epsilon}$ and aspartate 100 carboxylate CO_2^{γ} observed in the crystal structures of the unligated bovine FKBP12, human FKBP12–FK506 and FKBP12–rapamycin complexes and bovine FKBP12–rapamycin complex. (B) A region of the 2D soft CPD-H(N)CO spectrum of human FKBP12 recorded by using the pulse sequence of Figure 1 with the delay $\Delta = 5.5$ ms, together with (C) the [^{15}N, ^{1}H]-HSQC spectrum containing arginine guanidinium $^{15}N^{\epsilon}(^1H^{\epsilon})$ resonances and (D) the 2D H(C)CO_2 spectrum (Pellecchia et al., 1997b) containing aspartate carboxylate $^{13}CO_2{}^{\gamma}(^1H^{\beta})$ resonances. Resonances in (C) and (D) were assigned to individual residues based on the reported $^1H^{\epsilon}$ (C) and $^1H^{\beta}$ (D) shifts (Rosen et al., 1991; Xu et al., 1993). The two $^1H^{\beta}$ resonances that correlate with individual $^{13}CO_2$ in (D) are linked to each other with solid horizontal lines. The sole peak observed in (B) correlates the $^1H^{\epsilon}$ resonance of Arg 71 and $^{13}CO_2$ of Asp 100, as indicated with dashed lines, through the hydrogen bond-mediated $^{3h}J_{N\epsilon CO2\gamma}$ coupling. All spectra were recorded with acquisition times of $t_{2max}(^1H) = 128$ ms and $t_{1max}(^{13}C) = 32$ ms for (B), $t_{1\,max}(^{15}N) = 40$ ms for (C) and $t_{1max}(^{13}C) = 32$ ms for (D), respectively. 800 scans per t_1 increment for (B), 4 scans for (C), and 32 scans for (D) were used, which resulted in experimental times of 1 day, 30 min, and 3.2 h for respective spectra. The NMR samples contained either 3.1 mM $^{15}N/^{13}C$-labeled protein dissolved in 250 μL of 93%/7% H_2O/D_2O with a Shigemi microcell or 1.5 mM $^{15}N/^{13}C$-labeled protein dissolved in 500 μL of D_2O with 25 mM sodium acetate-d_3 at pH 5.0. NMR spectra were collected at 25 °C on a Varian Inova 600 MHz (^{1}H) instrument equipped with a z-axis pulsed field gradient probehead.

chains are generally more flexible than the backbone and share a shorter *effective* global correlation time. For the special case of the arginine side chain, the one-bond $^1J_{N\epsilon C\delta}$ coupling constant between the $^{15}N^{\epsilon}$ and $^{13}C^{\delta}$ spins is about 20 Hz, which is two times larger than the backbone sequential $^1J_{N\alpha}$ and $^2J_{NC\alpha}$ coupling constants (Bystrov, 1976). Consequently, the build-up of $2(^{15}N^{\epsilon})_{x,y}(^{13}C^{\delta})_z$ anti-phase coherence during the $^{15}N^{\epsilon} \leftrightarrow {}^{13}CO_2{}^{\gamma}$ defocusing/refocusing period in the HNCO-type experiments is much more efficient when the $^1J_{N\epsilon C\delta}$ coupling is active and the *J*-coupling mediated dipole–dipole (DD) relaxation is far more significant (Liu et al., 2000b). Thus, it is critical to efficiently decouple the arginine side chain $^{13}C^{\delta}$ spin to inactivate the $^1J_{N\epsilon C\delta}$ coupling during the entire $^{15}N^{\epsilon} \leftrightarrow {}^{13}CO_2{}^{\gamma}$ defocusing/refocusing period. Secondly, $^{15}N^{\epsilon/\eta}$ selective pulses are used in the $^1H^{\epsilon/\eta} \rightarrow {}^{15}N^{\epsilon/\eta}$ INEPT (Morris and Freeman, 1979) and the reverse elements to select magnetization transfer within the arginine guanidinium $^1H^{\epsilon/\eta}$–$^{15}N^{\epsilon/\eta}$ moiety and suppress resonances stemming from amides. The pulse sequence of the soft CPD-HNCO experiment with the description of magnetization transfer pathways outlined in the figure caption is shown in Figure 1.

Figure 2 shows a region of the 2D soft CPD-H(N)CO spectrum (B) of human FKBP12, together with the [^{15}N,^{1}H]-HSQC (C) and 2D H(C)CO_2 (D) spectra. The unique correlation signal in (B) that links Arg 71 $^{15}N^{\epsilon}(^1H^{\epsilon})$ and Asp 100 $^{13}CO_2{}^{\gamma}(^1H^{\beta})$ resonances clearly indicates the existence of the side chain–side chain N^{ϵ}–H···O=C^{γ} hydrogen bonding interaction in the Arg 71–Asp 100 salt bridge. The extremely weak intensity of this resonance prevents the quantification of this $^{3h}J_{N\epsilon CO2\gamma}$ coupling within a reasonable measuring time. However, in a previous publication, we used the 2D CPD-H(N)CO experiment (Liu et al., 2000b) to detect backbone N-H···O=C hydrogen bonds of human FKBP12 with the same sample under identical experimental conditions and the corresponding hydrogen bond-related resonances appeared much stronger than the resonance observed here. For 14 observed backbone N-H···O=C hydrogen bonds of human FKBP12, the average diatomic

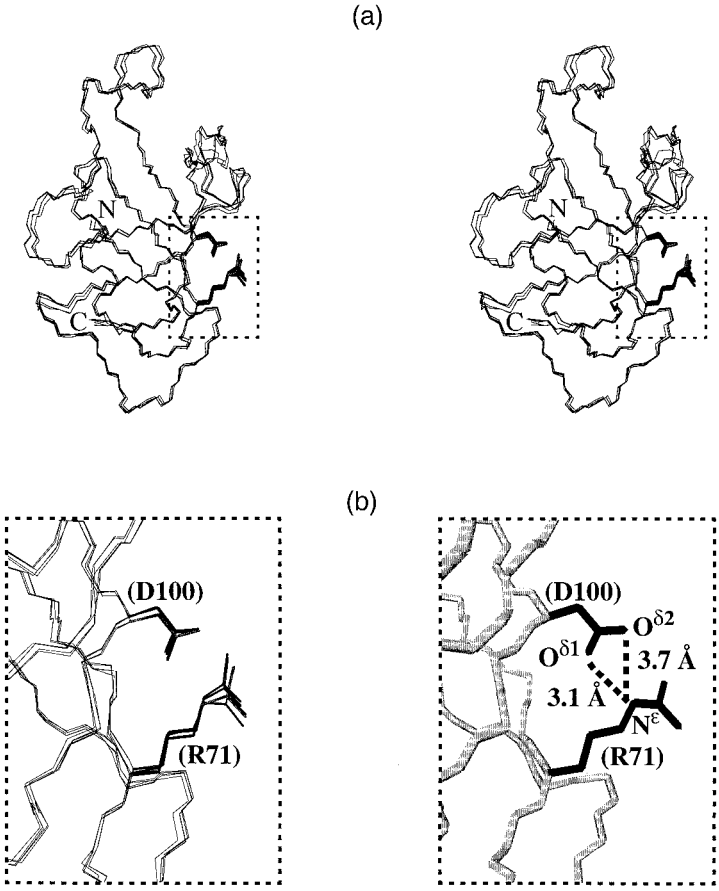

Figure 3. Stereoview of superposition of the crystal structure coordinates of unligated bovine FKBP12 (2.2 Å resolution, PDB accession code 1FKK), human FKPB12–FK506 complex-1 (1.7 Å resolution, PDB accession code 1FKF), human FKBP12–rapamycin complex (1.7 Å resolution, PDB accession code 1FKB), human FKBP12–FK506 complex-2 (1.7 Å resolution, PDB accession code 1FKJ), and bovine FKBP12–rapamycin complex (1.7 Å resolution, PDB accession code 1FKL). Protein backbones are represented with thin lines and R71 and D100 side chains with thick lines. The N- and C-termini are indicated. (b) Highlights of the side chains of the R71–D100 salt bridge (left) of the dashed region in (a) and the corresponding structural region of unligated bovine FKBP12 (right) with the backbone represented in grey cones and R71 and D100 side chains in solid cones. Diatomic distances of N^{ϵ}(R71)–O^{δ}(D100) are indicated accordingly.

distance between the backbone carbonyl oxygen and the amide nitrogen in the high resolution crystal structures of unligated FKBP12 (Wilson et al., 1995) and its complexes with FK506 and rapamycin (Van Duyne et al., 1991a,b, 1993; Wilson et al., 1995) is 2.9 Å. The corresponding distance between R71 side chain N^{ϵ} and one of the D100 carboxylate oxygens has a very similar value (see Figure 3). Interestingly, the X-ray structure B-factors for D100 carboxylate oxygens are very similar to those of amide nitrogens and carbonyl oxygens of the 14 backbone–backbone hydrogen bonds, but the B-factors of R71 N^{ϵ} in all crystal structures are about 30% larger. Given that the reported $^{3h}J_{NC'}$ coupling constants range from 0.25 to 0.92 Hz (Cordier and Grzesiek, 1999; Cordier et al., 1999; Cornilescu et al., 1999a), the $^{3h}J_{N\epsilon CO2\gamma}$ coupling constant of this Arg 71–Asp 100 salt bridge must be smaller than 0.2 Hz, consistent with more extensive local dynamics in protein side chains, although larger B-factors need not necessarily reflect more extensive dynamics in NMR solution structures.

Discussion

The locations of the arginine side chains and their proximity to the side chains of acidic residues are available from the published 2.2 Å resolution crystal structure of unligated bovine FKBP12 and 1.7 Å resolution crystal structures of human as well as bovine FKBP12 bound to FK506 and rapamycin. The side

chains are less well defined in the NMR solution structure of free human FKBP12 (Michnick et al., 1991) and hence the comparison was made with the higher resolution crystal structures of the free bovine FKBP12 and the FK506 and rapamycin bound forms. All six arginines are located on the surface of the protein with the guanidinium side chains of R13, R18, and R57 directed outwards towards the solvent, making hydrogen bonds to water. Salt bridges are formed between the guanidinium groups of the remaining arginines and the carboxylate groups of aspartate/glutamate residues, forming R40–E102, R42–D37 and R71–D100 pairs in all aforementioned crystal structures. Only the R71–D100 pair exhibits a hydrogen bond between a guanidinium H^{ϵ} donor and a carboxylate O^{δ} acceptor in all the crystal structures. Indeed, it is this H^{ϵ}-H$\cdots$O=C^{γ} hydrogen bond which was identified in the present NMR study of the free human FKBP12 in solution. The H^{η}, but not the H^{ϵ} arginine protons are involved in R42–D37 salt bridge formation with the N^{η}(R42)–O^{δ}(D37) distance ranging from 2.8 Å to 4.5 Å and the N^{ϵ}(R42)–O^{δ}(D37) distance is larger than 4.9 Å in all the crystal structures. Both the H^{ϵ} and H^{η} R71 protons are involved in the R71–D100 salt bridge formation, with the N^{ϵ}(R71)–$O^{\delta 1}$(D100) and $N^{\eta 2}$(R71)–$O^{\delta 2}$(D100) distances smaller than 3.1 Å. Despite its short distance, no hydrogen bond involving R71 H^{η} protons was observed in the present study. Since R71 N^{ϵ} and N^{η} atoms have similar B-factors in the crystal structures, the failure to detect the N^{η}H(R71)–O^{δ}=C(D100) hydrogen bond is likely due to the rapid exchange of R71 H^{η} protons with water. This conclusion is consistent with the broad H^{η} resonances in the [^{15}N,^{1}H]-HSQC spectrum (data not shown). Only one diatomic distance, $N^{\eta 2}$(R40)–$O^{\delta 1}$(E102), for the R40–E102 pair is smaller than 5.0 Å, indicating a possible weak salt bridge, if formed at all.

The H^{ϵ} proton of R71 resonates at 9.15 ppm, which is downfield from the remaining arginine H^{ϵ} protons that resonate between 6.9 and 7.6 ppm (Figure 2C). Such large downfield shifts are characteristic of hydrogen bond formation (Wagner et al., 1983) and provide further support for the N^{ϵ}-H$\cdots$O=C^{γ} hydrogen-bond stabilized salt bridge for the R71–D100 pair. Large downfield shifts of the arginine H^{ϵ} (and H^{η}) protons may serve as useful indicators of hydrogen-bonded salt bridge formation in solution, a conclusion subject to verification from coupling constant measurements of the type outlined in this study. A statistic search for arginine side chain $^{1}H^{\epsilon}$ chemical shifts from the full BioMagResBank archive leads to 13 outcomes that show low-field shifts larger than 9.10 ppm. Eight out of these results (BMRB accession numbers: 2539, 289, 3032, 395, 1037, 2069, 2066, 2067) have corresponding high resolution crystal structures in either free or complex forms with coordinates deposited in the Protein Data Bank. All theses arginines in the crystal structures form hydrogen-bonded Arg–Glu or Arg–Asp salt bridges with N^{ϵ}(Arg)–O^{ϵ}(Glu) or N^{ϵ}(Arg)–O^{δ}(Asp) diatomic distances shorter than 3.0 Å, except for the case of Eglin C in which $^{1}H^{\epsilon}$(Arg 51) forms a weak hydrogen bond with the backbone carbonyl of Gly 70. The generality of our coupling constant approach for monitoring hydrogen-bonded salt bridges in proteins must await experimentation on additional systems. A promising system involves the N-terminal domain of the 434 repressor which contains a single downfield-shifted H^{ϵ} proton, assigned to R10, resonating at $\approx$ 11.8 ppm (Pellecchia et al., 1997a). R10 forms a buried salt bridge with E35 in the 434 repressor and this pair is conserved amongst other prokaryotic and eukaryotic DNA-binding helix-turn-helix repressor proteins (Pervushin et al., 1996).

Conclusions

In summary, we have identified a *trans*-hydrogen bond *J*-coupling involving amino acid residue side chains in a 12 kDa protein. Although the measured scalar coupling constant appeared to be even smaller than its counterparts involving the backbone, such experiments should provide useful markers for monitoring hydrogen bonding interactions in the folded state of proteins and within the active sites of enzymes, as well as provide insights into aspects of molecular recognition at macromolecular interfaces.

Acknowledgements

This research was supported by NIH grant CA-46533 to D.J.P. and NSF grant MCB-9817376 to M.K.R. We thank Dr. L.T. Kakalis for preparing ^{13}C/^{15}N-labeled human FKBP12.

References

Bystrov, V.F. (1976) *Prog. NMR Spectrosc.*, **10**, 41–81.
Cordier, F. and Grzesiek, S. (1999) *J. Am. Chem. Soc.*, **121**, 1601–1602.

Cordier, F., Rogowski, M., Grzesiek, S. and Bax, A. (1999) *J. Magn. Reson.*, **140**, 510–512.
Cornilescu, G., Hu, J.-S. and Bax, A. (1999a) *J. Am. Chem. Soc.*, **121**, 2949–2950.
Cornilescu, G., Ramirez, B.E., Frank, M.K., Clore, G.M., Gronenborn, A.M. and Bax, A. (1999b) *J. Am. Chem. Soc.*, **121**, 6275–6279.
Dingley, A.J. and Grzesiek, S. (1998) *J. Am. Chem. Soc.*, **120**, 8293–8297.
Dingley, A.J., Masse, J.E., Peterson, R.D., Barfield, M., Feigon, J. and Grzesiek, S. (1999) *J. Am. Chem. Soc.*, **121**, 6019–6027.
Fischer, M.W.F., Majumdar, A. and Zuiderweg, E.R.P. (1998) *Prog. NMR Spectrosc.*, **33**, 207–272.
Geen, H. and Freeman, R. (1991) *J. Magn. Reson.*, **93**, 93–141.
Grzesiek, S. and Bax, A. (1992) *J. Magn. Reson.*, **96**, 432–440.
Grzesiek, S. and Bax, A. (1993) *J. Am. Chem. Soc.*, **115**, 12593–12594.
Harding, M.W., Galat, A., Uehling, D.E. and Schreiber, S.L. (1989) *Nature*, **341**, 758–760.
Hennig, M. and Geierstranger, B.H. (1999) *J. Am. Chem. Soc.*, **121**, 5123–5126.
Hennig, M. and Williamson, J.R. (2000) *Nucleic Acids Res.*, **28**, 1585–1593.
Jeffrey, G.A. and Saenger, W. (1991) *Hydrogen Bonding in Biological Structures*, Springer, New York, NY.
Kay, L.E., Ikura, M., Tschudin, R. and Bax, A. (1990) *J. Magn. Reson.*, **89**, 496–514.
Liu, A. (1999) *NMR Spectroscopy with Prion Proteins and Prion Protein Fragments*, Ph.D. Thesis No. 13234, ETH Zürich.
Liu, A., Majumdar, A., Hu, W., Kettani, A., Skripkin, E. and Patel, D.J. (2000a) *J. Am. Chem. Soc.*, **122**, 3206–3210.
Liu, A., Hu, W., Qamar, S. and Majumdar, A. (2000b) *J. Biomol. NMR*, **17**, 55–61.
Liu, A., Hu, W., Majumdar, A., Rosen, M.K. and Patel, D.J. (2000c) *J. Biomol. NMR*, **17**, 79–82.
Liu, A., Riek, R., Wider, G., Von Schroetter, Ch., Zahn, R. and Wüthrich, K. (2000d) *J. Biomol. NMR*, **16**, 127–138.
Majumdar, A., Kettani, A. and Skripkin, E. (1999a) *J. Biomol. NMR*, **14**, 67–70.
Majumdar, A., Kettani, A., Skripkin, E. and Patel, D.J. (1999b) *J. Biomol. NMR*, **15**, 207–211.
Marion, D., Ikura, M., Tschudin, R. and Bax, A. (1989) *J. Magn. Reson.*, **85**, 393–399.
McCoy, M. and Mueller, L. (1992) *J. Am. Chem. Soc.*, **114**, 2108–2112.
Meissner, A. and Sørensen, O.W. (2000) *J. Magn. Reson.*, **143**, 387–390.
Michnick, S.W., Rosen, M.K., Wandless, T.J., Karplus, M. and Schreiber, S.L. (1991) *Science*, **252**, 836–839.
Morris, G.A. and Freeman, R. (1979) *J. Am. Chem. Soc.*, **101**, 760–762.
Pellecchia, M., Wider, G., Iwai, H. and Wüthrich, K. (1997a) *J. Biomol. NMR*, **10**, 193–197.
Pellecchia, M., Iwai, H., Szyperski, T. and Wüthrich, K. (1977b) *J. Magn. Reson.*, **124**, 274–278.
Pervushin, K., Billeter, M., Siegal, G. and Wüthrich, K. (1996) *J. Mol. Biol.*, **264**, 1002–1012.
Pervushin, K., Ono, A., Fernández, C., Szyperski, T., Kainosho, M. and Wüthrich, K. (1998) *Proc. Natl. Acad. Sci. USA*, **95**, 14147–14151.
Rosen, M.K., Standaert, R.F., Galat, A., Nakatuska, M. and Schreiber, S.L. (1990) *Science*, **248**, 863–866.
Rosen, M.K., Michnick, S.W., Karplus, M. and Schreiber, S.L. (1991) *Biochemistry*, **30**, 3774–4789.
Scheurer, C. and Brüschweiler, R. (1999) *J. Am. Chem. Soc.*, **121**, 8661–8662.
Shaka, A.J., Keeler, J., Frenkiel, T. and Freeman, R. (1983) *J. Magn. Reson.*, **52**, 335–338.
Shaka, A.J., Barker, P.B. and Freeman, R. (1985) *J. Magn. Reson.*, **64**, 547–552.
Siekierka, J.J., Huang, H.Y., Poe, M., Lin, C.S. and Sigal, N.S. (1989) *Nature*, **341**, 755–757.
Van Duyne, G.D., Standaert, R.F., Karplus, P.A., Schreiber, S.L. and Clardy, J. (1991a) *Science*, **252**, 839–842.
Van Duyne, G.D., Standaert, R.F., Schreiber, S.L. and Clardy, J. (1991b) *J. Am. Chem. Soc.*, **113**, 7433–7434.
Van Duyne, G.D., Standaert, R.F., Karplus, P.A., Schreiber, S.L. and Clardy, J. (1993) *J. Mol. Biol.*, **229**, 105–124.
Wagner, G., Pardi, A. and Wüthrich, K. (1983) *J. Am. Chem. Soc.*, **105**, 5948–5949.
Wang, Y.X., Jacob, J., Cordier, F., Wingfield, P., Stahl, S.J., Lee-Huang, S., Torchia, D., Grzesiek, S. and Bax, A. (1999) *J. Biomol. NMR*, **14**, 181–184.
Wilson, K.P., Yamashita, M.M., Sintchak, M.D., Rotstein, S.H., Murcko, M.A., Boger, J., Thomson, J.A., Fitzgibbon, M.J., Black, J.R. and Navia, M.A. (1995) *Acta Crystallogr.*, **D51**, 511–521.
Xu, R.X., Nettesheim, D., Olejniczak, E.T., Meadows, R., Gemmecker, G. and Fesik, S.W. (1993) *Biopolymers*, **33**, 535–550.